17th World Conference on Earthquake Engineering, 17WCEE
Sendai, Japan - September 13th to 18th 2020

INVESTIGATION ON THE COLUMN SHEAR FAILURE DUE TO THE LOCAL INTERACTION WITH MASONRY INFILLS IN RC FRAMES

M.T. De Risi[1], C. Del Gaudio[2], P. Ricci[3], G.M. Verderame[4], G. Manfredi[5]

[1] *Assistant Professor, University of Naples Federico II, Department of Structures for Engineering and Architecture, beneficiary of an AXA Research Fund Postdoctoral grant, mariateresa.derisi@unina.it*
[2] *Post-Doctoral Researcher, University of Naples Federico II, Department of Structures for Engineering and Architecture, carlo.delgaudio@unina.it*
[3] *Assistant Professor, University of Naples Federico II, Department of Structures for Engineering and Architecture, paolo.ricci@unina.it*
[4] *Associate Professor, University of Naples Federico II, Department of Structures for Engineering and Architecture, verderam@unina.it*
[4] *Full Professor, University of Naples Federico II, Department of Structures for Engineering and Architecture, gamanfre@unina.it*

Abstract

RC buildings designed for gravity loads only or according to obsolete seismic codes are widespread worldwide also in seismic prone areas. Numerical and experimental studies highlighted that the presence of masonry infills in Reinforced Concrete (RC) frames leads to the increase in their lateral strength and stiffness. Nevertheless, post-earthquake observed damage showed that infills can also cause potential brittle failures due to the local interaction with structural elements, thus producing a limitation of deformation capacity of the surrounding frame, especially in sub-standard frames. A reliable modelling approach for the assessment of the as-built condition and the design of retrofitting solutions about this kind of failure is still needed.

Experimental tests on RC frames designed according to obsolete technical codes and infilled with clay bricks have been performed and presented in this work. The frames have been cyclically loaded with a quasi-static displacement pattern to simulate the seismic action. The experimental occurrence of significant shear damages is discussed, and the main outcomes are described, commented and compared to each other. The work lastly provides further data and modelling remarks towards a reliable numerical simulation of local shear interaction phenomena between infills and RC frames.

Keywords: RC buildings; shear failure; local shear interaction; masonry infills; experimental results

1. Introduction

RC buildings designed for gravity loads only or according to obsolete seismic codes are widespread worldwide also in seismic prone areas. Numerical and experimental studies highlighted that the presence of masonry infills in Reinforced Concrete (RC) frames leads to the increase in their lateral strength and stiffness. Nevertheless, post-earthquake observed damage showed that infills can also cause potential brittle failures due to the local interaction with structural elements, thus producing a limitation of deformation capacity of the surrounding frame, especially in sub-standard frames. A reliable modelling approach for the assessment of the as-built condition and the design of retrofitting solutions about this kind of failure are still needed.

During last decades, several experimental studies investigated the seismic behavior of RC frames with infills, but a few of them investigated the effects of the interaction between the infill panel and surrounding elements resulting in brittle failure mechanisms such as shear failure in RC columns (e.g., [1], [2]), above all for infills made up of hollow clay bricks, very widespread in the Mediterranean region [3]. The topic certainly deserves a deeper investigation, both about *(i)* the best infill modelling strategy and, consequently, the definition of the column shear demand due to the interaction, and *(ii)* the more suitable shear strength model to be adopted for the columns.

Experimental data about infilled RC frames have been the support for analytical modelling efforts since late 1970s'. Infills have been generally modelled by means of quite complex FEM micro-modelling approaches or simpler single- or multi-struts (reacting only in compression) approaches. Nevertheless, even recently, there is lack of unanimity about the best modelling approach among the various literature proposals (e.g., [4]-[6]), above all about the column-infill shear interaction modelling strategy, since, obviously, the shear demand in the surrounding RC members strictly depends on the modelling strategy to reproduce the infill response. More specifically, about the shear failure modelling in non-ductile RC frames, some standards propose simplified procedures aimed at considering the effects of the interaction between infill panels and surrounding RC elements. These procedures usually consider a concentrated load on the column (or beam) equal to the horizontal (or vertical) component of the resultant of the stresses along the loaded diagonal of the infill panel. Among codes, some practice-oriented prescriptions are present in the American ASCE/SEI 41-06 [7], which suggested to model the infill as a single eccentric strut in compression. On the contrary, the most recent Italian technical standards ([8],[9]) do not provide any suggestion for the modelling and the assessment of the local interaction phenomena in the case of panels adjacent to column/beam elements. About research studies from literature, the issue of shear failure modelling in non-ductile RC frames due to local interaction with infill elements has been investigated with different approaches during the last years (e.g., [10]-[13], among others). Multiple-strut approaches are often suggested in these studies, generally proposing to model the infill by a minimum of one-strut - eccentrically placed with respect to the infill diagonal, like suggested in the ASCE-SEI/41 [7] - to a maximum of two or three struts (per loading direction), basically different for the position of the loading points on the adjacent columns, the ratio of the total infill lateral load adsorbed by each strut, and for the struts inclination. The number of struts, their positions, and their width have to be carefully selected to reliably reproduce the stress demand they induce and the strength and deformability contribution of the panel to the infilled RC frame.

Another key issue for the shear local interaction modelling is the adequacy and the applicability of the usually adopted shear capacity models in capturing the shear-controlled behaviour of a RC member adjacent to an infill panel. All the proposals from codes and literature mentioned above suggest using the model by Sezen and Moehle [14], also adopted in the current American code ASCE-SEI/41 [15]. This model assumes a shear strength degradation due to the inelastic ductility demand, as typical in mono-dimensional columns/beams, and can be applicable within a certain range of slenderness ([2; 4]). In the case of very "squat" portions of columns, as those generated by the limited infill-to-column contact length, a shear strength degradation due to an increasing flexural demand appears not totally meaningful. Therefore, the model by Sezen and Moehle [14], if applicable, should be applied without any strength degradation. Alternatively, a different "family" of shear strength models should be adopted, degrading with the shear

crack opening demand or, from a predictive standpoint, with the strain demand, instead than with the flexural inelastic ductility demand [3].

In this research work, experimental tests on RC frames designed according to obsolete technical codes and infilled with hollow clay bricks are presented and analysed to provide a contribution in understanding which model for shear demand and for shear capacity are more adequate when the local shear interaction problem is faced up. The 2:3-scaled tested frames have been cyclically loaded with a quasi-static displacement pattern to simulate the seismic action. The experimental occurrence of shear failure is discussed, and the main outcomes are analysed.

2. Experimental campaign description

The experimental campaign carried out and presented in this work is described in this section, in terms of specimens' main features and material properties (section 2.1), and experimental setup (section 2.2).

2.1 Specimens description

Four one-bay one-story 2:3-scaled RC frames infilled with hollow clay masonry bricks have been tested. Clear bay length and story height are equal to 2.30 m and 1.83 m respectively (see Fig. 1). Cross section dimensions of columns and beams are 20×20 cm and 20×27 cm, respectively. Deformed bars were used for longitudinal reinforcement. Columns were fixed in a 0.40×0.40×3.90 m foundation beam.

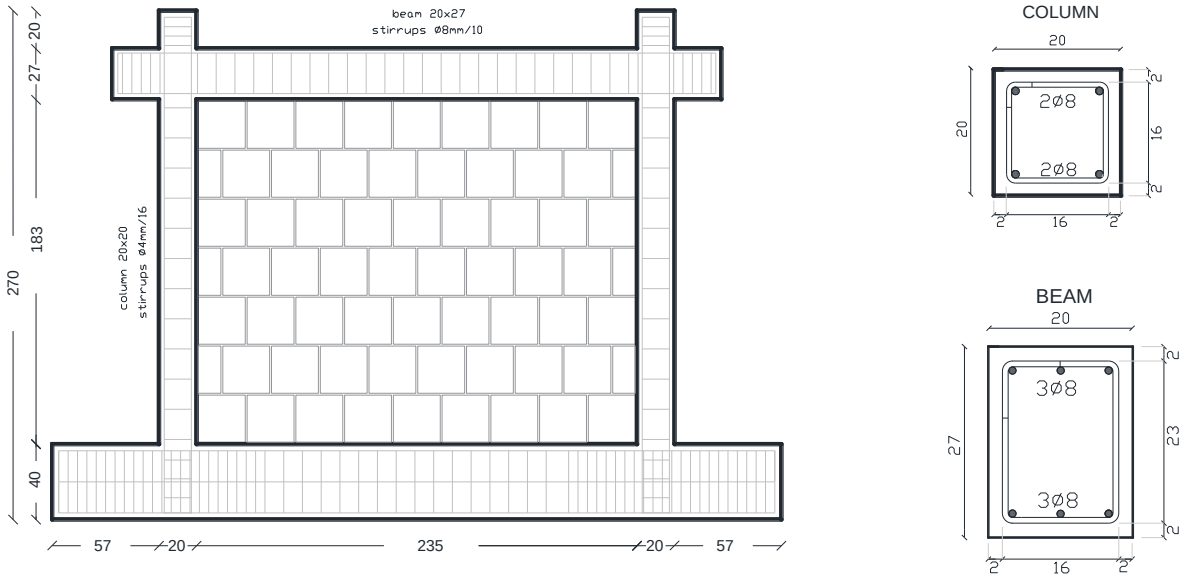

Fig. 1 – Specimens details (dimensions in cm)

The RC frames are all identical; they were designed for gravity loads only, according to the obsolete Italian code R.D.1939 [16], to be representative of low-standard existing RC buildings, and they resulted in a weak column-strong beam hierarchy. Each frame has been filled with a hollow clay masonry infill panel. The infill panel was built in total connection with the concrete frame along the four edges through mortar joints (specimens named with the suffix "4E") or with a gap from the top beam (specimens named with the suffix "3E") to simulate defects in the actual realization in a real building. Infill walls thickness (t_w) is equal to 120 mm (specimens named "120_") or 150 mm (specimens named "150_"), realized with 250×250×120 mm^3 or 250×250×150 mm^3 clay hollow bricks with a nominal void percentage equal to 60%. 1 cm thick horizontal and vertical courses of mortar are present among bricks, which are placed with the holes in the horizontal direction.

About material properties adopted for this experimental campaign, concrete compressive strength was equal to 11.7±1.1 MPa, namely representative of low-standard existing RC buildings in the Mediterranean area. Class B450C reinforcing steel (with a nominal tensile yielding strength of 450 MPa) has been used for 8-mm diameter longitudinal and transverse reinforcement bars. Stirrups in columns were constituted by 4-mm diameter reinforcing bars with a 90° hook, as typical in existing RC buildings (considering a 2:3 scale factor), with a mean yielding strength equal to about 420 MPa (and an ultimate strength of 569 MPa), thus obtaining a transverse reinforcement mechanical percentage in columns equal to 2.8%.

Tensile and compressive tests have been performed on mortar used for the infill panels according to ASTM C109 / C109M-16a standard [17]. Three mortar prisms have been prepared for each specimen, twelve mortar prisms overall. The related mechanical properties and their coefficients of variation are shown in Table 1. Nominal bricks' compressive strength in the direction parallel to the holes is also shown in Table 1, as provided by the material supplier. It can be noted that thicker bricks (with 150 mm thickness) have lower compressive strength (about 40%) of the thinner bricks (with 120 mm thickness) adopted in this study.

Table 1– Infills materials properties

Material property	Symbol	Mean value	CoV
Mortar compressive strength	$f_{m,c}$	9.35 MPa	12.4%
Mortar tensile strength	$f_{m,t}$	2.22 MPa	0.64%
brick compressive strength* t_w=120 mm	$f_{b,120}$	5.95 MPa	-
brick compressive strength* t_w=150 mm	$f_{b,150}$	2.26 MPa	-

(*) compressive strength parallel to the holes' direction - nominal values provided by the material supplier

2.2 Loading setup and instrumentation

The loading setup is shown in Fig. 2. The specimen is first rigidly fixed to the strong floor of the laboratory by means of two steel stiff beams with pre-stressed rods and horizontal steel constrains. The vertical hydraulic jacks located on the top columns applied a constant level of axial load equal to 47 kN, corresponding to an axial load ratio of 10%. Two stiff steel plates were located at the top beam ends and were connected to each other by means of pre-stressed rods. Then a hydraulic actuator – externally constrained to a reaction cantilever – applies a cyclic displacement (d_{IP}) history at one top beam end, by progressively increasing the applied drift until pre-defined target drift levels (as shown in Table 2) in displacement control. Three push-pull cycles have been performed for each applied drift level, starting with the pulling (negative) direction. Note that the IP drift values are calculated as the ratios between IP displacements and the distance of the beam centerline from the top face of the foundation beam (i.e., 196.5 cm).

The monitoring system is shown in Fig. 2. One control wire potentiometer (WP) has been used to measure the actual applied displacement in the beam centerline (d_{IP}), and one Linear Variable Displacement Transducer (LVDT) provided eventual horizontal sliding of the foundation beam. Additionally, two WPs monitored the deformation of the panel diagonals; four vertical LVDTs (LVDTv) have been placed at the column base to measure the fixed-end rotation deformability contribution. Lastly, for each (top) column, a monitoring system made up of 4 horizontal LVDTs (LVDTh) and four vertical linear potentiometer (LPs) have been located to measure the horizonal and the vertical components of the expected shear cracks in those regions. Additional two horizontal LVDTs measure the horizontal displacement of a column point (for each column) at about 60 cm distance from the beam-to-column interface.

Note that during the test, the actual d_{IP} monitored by the control WP at the beam centerline results a bit lower than the pre-defined assigned displacement level, mainly due to the (slight) deformability of the reaction cantilever. Therefore, the following description of the experimental results will refer to the actual drift levels (see section 3).

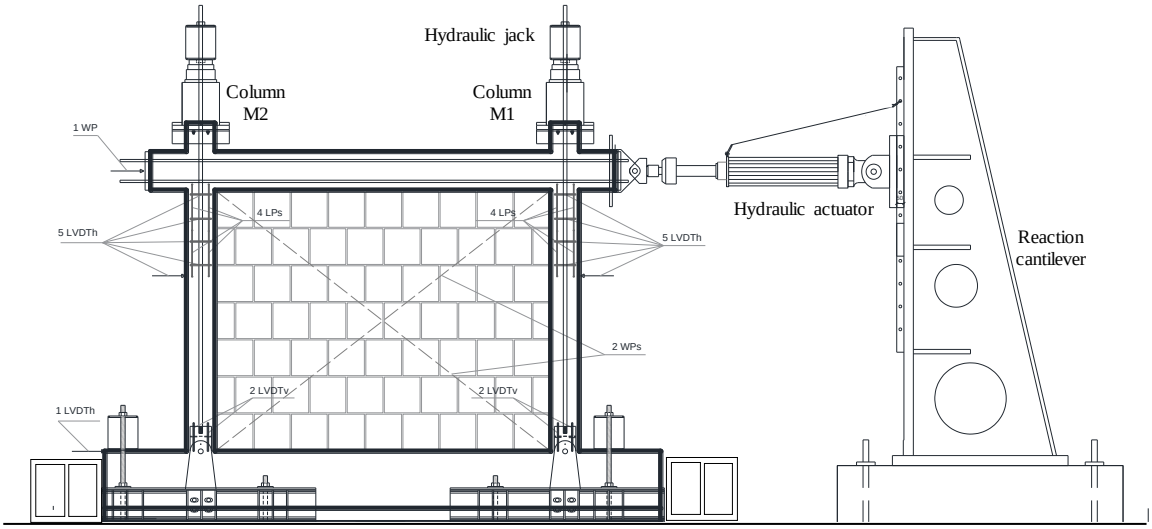

Fig. 2 – Experimental setup and monitoring system

Table 2 – Applied loading history

Cycle	**(-)**	1	2	3	4	5	6	7	8	9	10	11	12	13
Drift	**(%)**	0.025	0.05	0.1	0.2	0.4	0.8	1.2	1.6	2	2.4	2.8	3.4	4
d_{IP}	**(mm)**	0.49	0.98	1.97	3.93	7.86	15.72	23.58	31.44	39.3	47.16	55.02	66.81	78.60

3. Experimental results

In this section, the main experimental results are shown and commented, in terms of base shear (V_{base})-drift cyclic response (see Fig. 3a and Fig. 4a) and damage evolution. The final damage state for each specimen is reported in Fig. 3b and Fig. 4b.

3.1. Specimen 120_4E

This specimen was characterized by an infill panel thickness equal to 120 mm, well connected with the frame along the four edges.

During the very first steps of this test, until an actual applied drift level equal to 0.07% no significant cracks appeared, and only slight detachment of the infill panel from the surrounding frame was observed. At 0.15% drift, very slight cracks appeared in the infill top corner (close to M2 column), which became evident at the following cycle (at 0.32% drift). At 0.32% drift, additionally, first horizontal sliding between the panel and the top beam were observed, slight diagonal cracks developed in the infill panel, with about 60° inclination with respect to the horizontal direction, starting from the top corners, and hairline cracks occurred in the top M1 column, with about 30° inclination with respect to the horizontal direction. In the following cycle, the peak load was reached, namely $V_{base} = V_{max,+} = +116.5$ kN at +0.66% and $V_{base} = V_{max,-} = -108.5$ kN at -0.57%. At this stage, existing diagonal cracks in the panel and inclined cracks at the top columns became more evident; an additional crack occurred in column M2 (where the third stirrup was located, at about 32 cm from the column-beam interface) with about 45° inclination. Such cracks in top columns appeared in the ascending phase of the global response, proving the existence of a shear interaction due to the lateral infill action on the columns. In the following cycle, at drift = 1.1%, additional cracks developed in the panel, parallel to the first ones, and corner crushing at both the infill top corners occurred, with the detachment and the overturning of some external bricks' tiles; shear cracks in top column became wider. In the following sub-cycles at the same drift level, additional tiles overturned from the whole last row of bricks. When the drift level equal to about 1.5% is intended to be applied, in the positive (pushing) direction, a

sudden strength drop was observed at 1.1% drift (see red star in Fig. 3a), followed by a clear intra-cycle softening until the imposed drift level (1.5%). At this sub-cycle, an evident sliding along the crack surface was observed at the top of M1 column, together with a sudden elongation of the hydraulic jack located on that column (see section 4), thus highlighting the born of a shear failure and the subsequent losing of column axial load carrying capacity. A last sub-cycle in the negative direction was performed and the test was stopped, when the maximum strength decay with respect to the maximum achieved V_{base} was equal to 57%.

3.2. Specimen 120_3E

This specimen was characterized by an infill panel thickness equal to 120 mm, well connected with the frame only along three edges; about 3 cm gap was present between the infill panel and the top beam.

During the very first steps of this test, the V_{base}-drift response presented an elastic behavior less stiff than the previous test (as it will be discussed in the next section), as expected due to the weaker degree of connection between the frame and the panel. At the III cycle, the detachment of the panel from the columns was observed, with visible cracks in the top corner mortar bed joints during the IV cycle. At about 0.33% drift, the total detachment of about four rows of masonry bricks from the columns was evident, and hairline horizontal cracks appeared at the columns' ends.

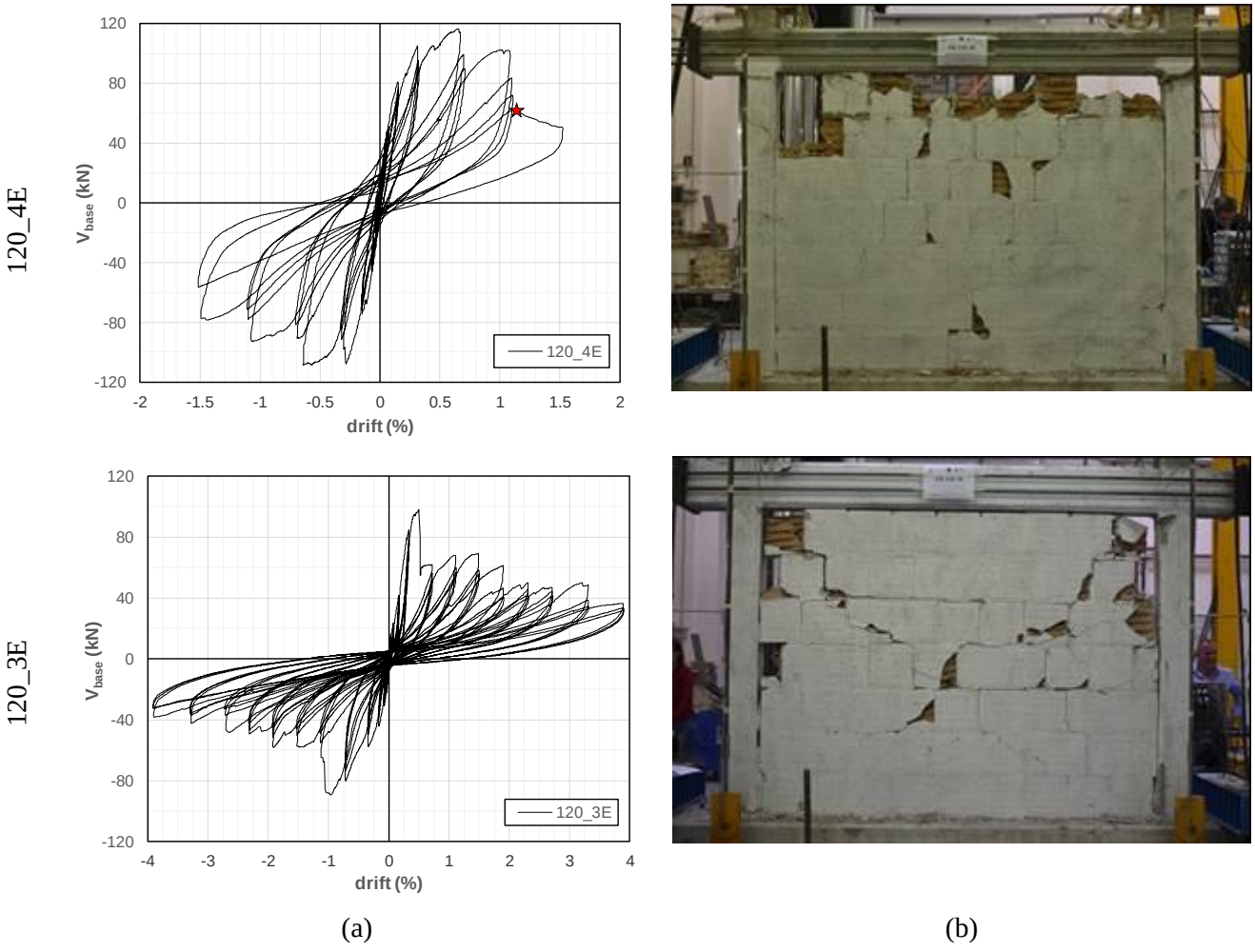

(a) (b)

Fig. 3 – Experimental results for specimens with t_w= 120 mm: base shear-drift cyclic response (a); final damage state (b)

At the following drift level, when 0.8% drift was intended to be applied, a significant diagonal crack appeared in the panel during the pushing phase (positive direction), thus producing a clear strength drop at

drift = +0.5%, and a hairline inclined crack occurred at the top M1 column; a slight inclined crack also appeared in column M2 (in pulling direction) at about 30 cm from the beam-to-column interface. The maximum V_{base} was achieved at +0.5% drift in the positive direction ($V_{max,+}$ = 97.7 kN). In the negative loading direction, the maximum base shear was achieved at -0.94% drift. At this stage, in the pull-direction, a clear crack was born along the panel diagonal, together with the a slight crack in top column M2, and a significant strength drop was observed also in this direction (see Fig. 3b). Vice-versa, in the push-direction at the same applied drift level, the widening of the existing diagonal crack in the infill was observed, with some bricks crushing in the center of the panel and in the top corner in contact with the column M1, where a clear (diagonal) shear crack was observed (with about 60° inclination with respect to the horizontal direction).

In the following cycles, exiting cracks in the infill progressively became wider, clearly isolating a roughly triangular portion of infill in the upper portion of the panel, which became free to move rotating around the infill central point and, thus nullifying the increment of its horizontal action on the adjacent columns. Therefore, in the columns' ends mainly horizontal cracks increased their width, whereas, no further development of diagonal shear cracks was observed or measured, thus producing a preeminent flexural behavior of the RC frame (with the flexural hinging of columns highlighted by horizontal cracks along the columns base side) from 1.6% drift to the end of the test (at about 4% drift). Obviously in this case, due to the contact length between the bottom portion of the infill and the column, the column clear length resulted lower than its total length. An almost constant residual strength was reached of about 40 kN, namely less than 50% of the maximum achieved base shear, and more than the expected plastic shear of the frame in the hypothesis of plastic hinging at the columns (weaker than beam)' ends.

3.3. Specimen 150_4E

This specimen was characterized by an infill panel thickness equal to 150 mm, well connected with the frame along the four edges.

The initial behavior of this specimen was roughly elastic until about 0.1% drift; at drift = 0.13%, first detachment of the panel from the column was observed; additionally, stepwise cracks appeared in the infill with about 60° inclination with respect to the horizontal direction, starting from the top M2 column corner, where a hairline sub-horizontal crack at the beam-column corner appeared. At the following cycle, in the pulling direction, a further crack appeared on the panel, parallel to the first one, and existing crack on the top of M2 column increases its inclination and width; the peak load was achieved in this direction at -0.31% drift ($V_{max,-}$ = -111.2 kN). In the opposite loading direction, cracks appeared in the panel almost symmetrically with respect to the vertical centerline, as expected, together with two slight inclined cracks on the top of M1 column; peak load was achieved in this direction, at 0.19% drift ($V_{max,+}$ = 119.2 kN). Slight horizontal cracks also appeared at the columns' base, at about 30 cm from the foundation beam. During the following step, at about 0.67% drift, further cracks developed in the panel in both directions, further detachment from the column and corner crushing in the top corners were observed in the infill, together with the enlarging of existing inclined cracks in top columns. Such cracks reasonably highlight the existence of a local shear interaction due to the horizontal action of the infill that leads to the violation of the cracking strength in the columns. Nevertheless, from about 1% drift to the end of the test, the infill panel progressively crushed in the top corners, where some bricks overturned, thus nullifying the lateral shear action on the top of the columns, where existing cracks evolved in flexural cracks (sub-horizontally) for increasing displacement demand, and further horizontal cracks developed along the column M2 and in the center of the column M1. Between 3% and 4% drift, at the bottom of both columns, about 45° inclined cracks appeared, becoming more evident (about 3 mm width) at the end of the test.

3.4. Specimen 150_3E

This specimen was characterized by an infill panel thickness equal to 150 mm, well connected with the frame along only three edges; about 3 cm gap was present between the infill panel and the top beam.

For this test, until 0.08%, only the detachment of the infill panel from the columns was observed. At about 0.2%, in the pulling (negative) direction a first hairline sub-horizontal crack appeared on the top

column M2. At about 0.3% drift, a further slight inclined crack appeared on the top of M2 column, whereas the existing crack became wider (during positive loading direction), and a first slight shear crack occurred on the top of M1 column (during the positive loading direction); these cracks on columns become progressively wider during the following sub-cycles at the same drift level. A slight crushing of some brick units close to the column M1 occurred during the pushing sub-cycles. At this stage, the peak load was reached in the negative loading direction, $V_{base} = V_{max,-} = -61.9$ kN. During the following cycle, at about 0.8% of applied drift, in the negative direction, the crushing of the infill corner was observed and the existing cracks in column M2 increased their width and evolved in sub-vertical direction, producing an intra-cycle softening (see Fig. 4a from -0.5% to -0.8% drift) on the global response. For the same drift level, in the positive direction, a further widening of the diagonal shear crack on the top column M1 is observed and the maximum load is achieved ($V_{base}= V_{max,+}= 77.8$ kN). Lastly, at about 1.2% drift, in the pulling (negative) direction, shear crack in M2 column further increased its width, and a visible sliding along the crack surface between the top and the bottom portion of the column was observed (red star in negative quarter in Fig. 4a); whereas, in the pushing (positive) direction, the shear damage in the top M1 column evolved in the losing of column axial load carrying capacity, with a sudden intra-cycle softening between 0.95% and about 1.1% (red star in positive quarter in Fig. 4a), when the test was prematurely stopped due to the sudden significant elongation of the hydraulic jack on the top M1 column (see section 4).

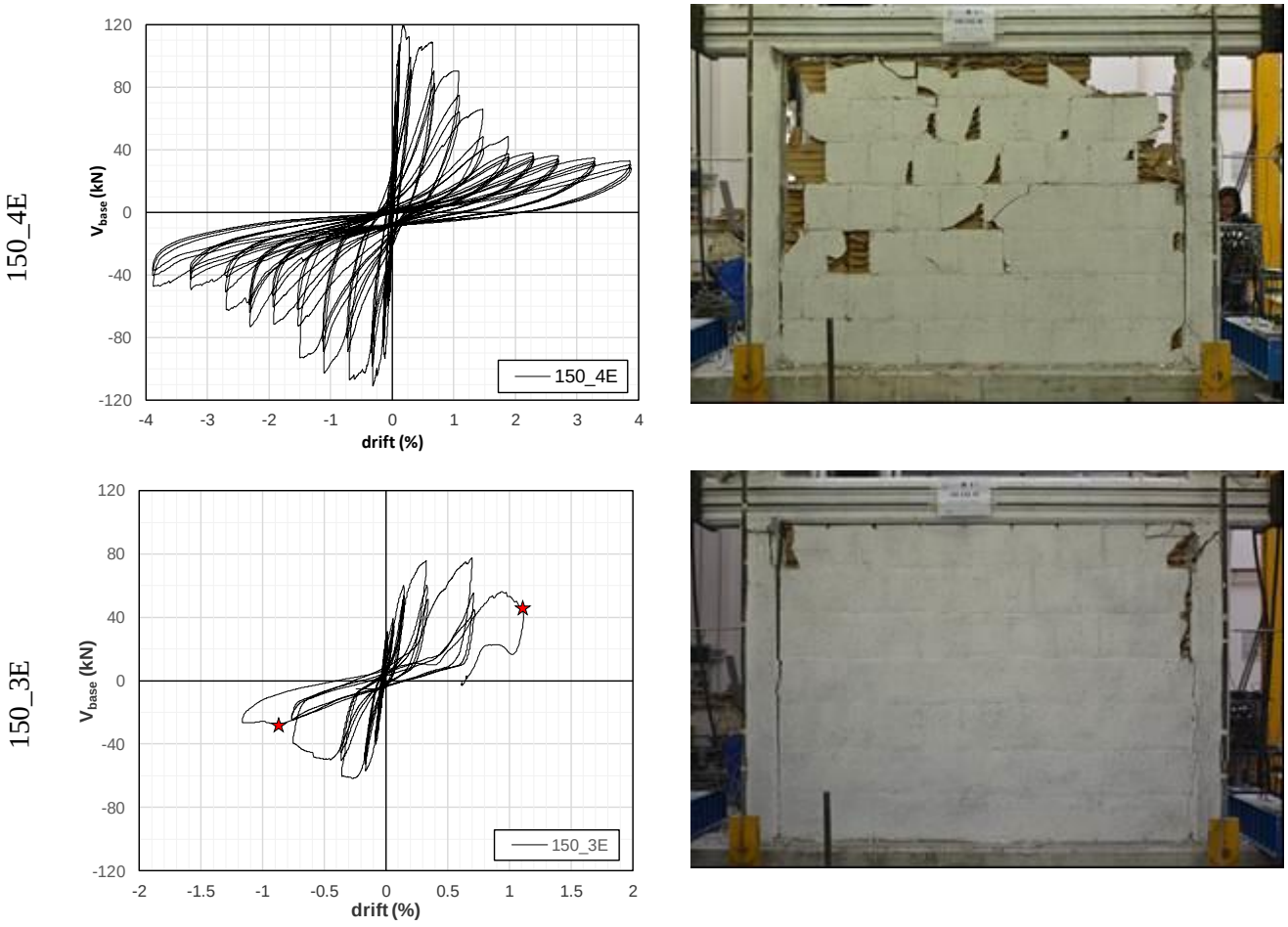

(a) (b)

Fig. 4 – Experimental results for specimens with t_w= 150 mm: base shear-drift cyclic response (a); final damage state (b)

At the end of the test, the infill panel appears only slightly cracked, with some crushing in the top corners, and totally detached from the surrounding columns; whereas the initial top gap between the infill

and the top beam is almost totally closed (see Fig. 4b) due to the sliding of the top beam with respect to the lower portion of the M1 column, along the main identified shear crack. The final global response results clearly asymmetric, due to the described evolution of shear cracking and failure in columns, and maximum achieved lateral load significantly lower (about 60%) than the maximum load achieved in the 150_4E specimen, as discussed in the next section.

4. Comparisons and preliminary remarks on modelling issues

The experimental results described above are compared to each other in this section. A first comparison can be carried out in terms of V_{base}-drift envelopes (as shown in Fig. 5), maximum base shear in both loading directions and related drift levels (as reported in Table 3).

It can be noted that the initial lateral stiffness of specimens infilled with thicker bricks (150 mm) is higher than the corresponding frames infilled with 120 mm bricks. Additionally, when infills are well connected along all the four edges with the frame (cases "4E"), the initial stiffness is higher than the corresponding cases "3E", as expected. On the other hand, for the "4E" specimens, the maximum achieved lateral load is almost the same for both the infill thickness, mainly due to the lower compressive strength (about 40%) of the thicker bricks (150 mm) with respect to the thinner bricks (120 mm), as shown in Table 1, which compensates for the higher thickness (and, consequently, the higher infill resisting area). If the cases "3E" are considered, the specimen with the higher bricks thickness shows even lower maximum base shear with respect to the case of 120 mm infill thickness, likely due to the very different behavior (ductile versus brittle) which characterized these two specimens, as described in the previous section.

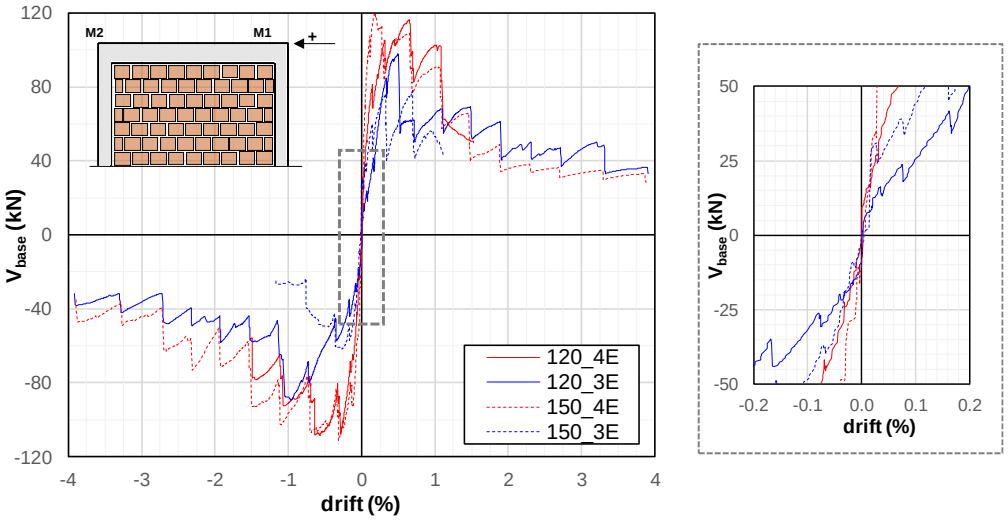

Fig. 5 – Comparison of experimental envelopes

Table 3 – Summary of the main experimental results

Test ID	$V_{max,+}$ (kN)	$V_{max,-}$ (kN)	$drift_{Vmax,+}$ (%)	$drift_{Vmax,-}$ (%)	$drift_{SC}$* (%)	$drift_{IAF}$** (%)
120_4E	116.5	-108.5	0.66	-0.57	±0.32	-/+1.1
120_3E	97.7	-89.4	0.50	-0.96	±0.50	-
150_4E	119.5	-111.2	0.19	-0.31	±0.31	-
150_3E	77.8	-61.9	0.70	-0.28	±0.30	-0.9/+1.1

(*) SC = first column shear cracking; (**) IAF = incipient axial failure

Additional details should be carried out about shear damage in columns already described in the previous section. Table 3 summarizes the drift values at which first column shear cracking (SC) was observed and, for specimens with a brittle failure, the drift values at which a clear evidence of a significant sliding of the two portions of the damaged column along the crack surface occurred. A clear evidence of such "incipient axial failure" (IAF) condition can be observed in Fig. 6 and Fig. 7 for specimens 120_4E and 150_3E, respectively. Such figures show the evolution of the hydraulic jack elongation acting on the columns, and the parameter Δ_h with the applied drift, where Δ_h is the difference between the horizontal displacement measured at the beam centerline and the horizontal displacement of a column point located at about 60 cm distance from the column-to-beam interface. Therefore, Δ_h is roughly proportional to the total horizontal component of the shear cracks developed within the first 60 cm from the column-to-beam interface. Fig. 6 shows that, for the test 120_4E, a sudden increment in Δ_h occurred at 1.1% (defined as the IAF point) for column M1 - corresponding to a sudden elongation of the hydraulic jack - and a residual value of Δ_h equal to 7.5 mm is measured at the end of the test for both the columns, as also visible from their final damage state (Fig. 6). Similarly, Fig. 7 shows the same information for the specimen 150_3E, where the residual Δ_h at the end of the test is more than 2 cm for column M1.

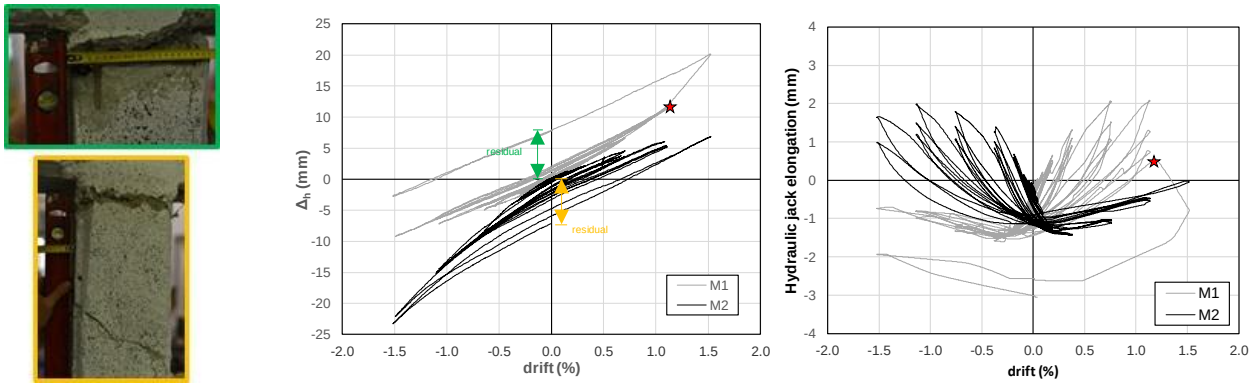

Fig. 6 – Specimen 120_4E: shear cracks horizontal component; damage state of the top columns at the end of the test (red star = "IAF")

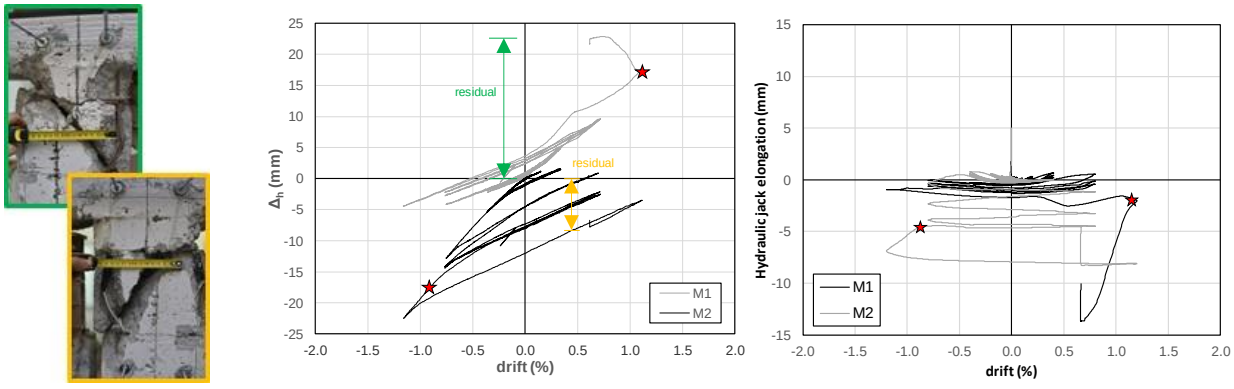

Fig. 7 – Specimen 150_3E: shear cracks horizontal component; damage state of the top columns at the end of the test (red star = "IAF")

It can be remarked that all the specimens were interested by a shear interaction phenomena between the panel and the columns that leads to, at least, a significant shear damage of columns, due to the low quality of the concrete, the low percentage of columns transverse reinforcement (as typical of existing buildings), and the lateral action of the panel concentrated in a small portion of the column. As a matter of fact, the presence of the infill, as well-know from the literature (see section 1), leads to the formation of

squat columns in the contact length with the compressed portion of the infill panel, thus magnifying the shear action that columns should be able to sustain. This means that shear models specific or, at least, applicable also to squat columns, should be adopted to reliably catch the column shear capacity (as pointed out also in [3]).

Moreover, it can be observed, particularly for specimens 120_4E and 150_3E, that column shear failure likely occurred between the peak load of the lateral response and the end of the test, namely in the descending branch of the global response, when, likely, the infill panel is reducing its total horizontal action. This means that a multi-strut model (like those suggested in [10] or [13], among others) is the best candidate modelling strategy for infills to numerically reproduce the local shear interaction, since, on the contrary, a single-strut model (even if eccentrically placed, like ASCE-SEI 41 [7] suggestion) can only detect column shear failure in the ascending phase of the infill response. Further future studies will be devoted to numerically reproduce the presented experimental results in agreement with these main remarks.

5. Conclusions

Reinforced Concrete (RC) buildings designed for gravity loads only or according to obsolete seismic codes are widespread worldwide also in seismic prone areas. Post-earthquake observed damage showed that infills can cause potential brittle failures due to the local interaction with structural elements, thus producing a limitation of deformation capacity of the surrounding frame, especially in sub-standard frames. A reliable modelling approach for the assessment of the as-built condition and the design of retrofitting solutions about this kind of failure is still needed.

In this work, four experimental tests on 2:3-scaled RC frames have been presented and analysed to provide a contribution in understanding which model for shear demand and for shear capacity are more adequate when the local shear interaction problem is faced up. The RC frames were all identical; they were designed for gravity load only, according to the obsolete Italian code R.D.1939 [16], to be representative of low-standard existing RC buildings, and they resulted in a weak column-strong beam hierarchy. Each frame has been filled with a hollow clay masonry infill panel. The infill panel was built in total connection with the concrete frame along the four edges through mortar joints (specimens named with the suffix “4E”) or with a gap from the top beam (specimens named with the suffix “3E”) to simulate defects in the actual realization in a real building. Infill walls thickness (t_w) was equal to 120 mm (specimens named “120_”) or 150 mm (specimens named “150_”). The specimens have been cyclically loaded with a quasi-static displacement pattern to simulate the seismic action. The experimental occurrence of shear failure has been discussed, and the main outcomes analysed.

It was found that all the specimens were interested by a shear interaction phenomena between the panel and the columns that lead to, at least, a significant shear damage of columns, due to the low quality of the concrete, the low percentage of columns transverse reinforcement (as typical of existing buildings), and the lateral action of the panel concentrated in a small portion of the column. As a matter of fact, the presence of the infill, as well-know from the literature, leads to the formation of squat columns in the contact length with the compressed portion of the infill panel, and, thus, to the necessity of shear capacity models specific or, at least, applicable also to squat columns. Moreover, it was observed, particularly for specimens 120_4E and 150_3E, that column shear failure likely occurred between the peak load of the lateral response and the end of the test, namely in the descending branch of the global response, when, likely, the infill panel is reducing its total horizontal action. This means that a multi-strut model should be used to model infills to numerically reproduce the local shear interaction, since a single-strut model can only detect column shear failure in the ascending phase of the infill response. Further future studies will be devoted to numerically reproduce these experimental results in agreement with the main modelling remarks commented in this work.

6. Acknowledgements

This work was developed under the support of AXA Research Fund Post-Doctoral Grant "Advanced nonlinear modelling and performance assessment of masonry infills in RC buildings under seismic loads: the way forward to design or retrofitting strategies and reduction of losses", ReLUIS-DPC 2019-2021 funded by the Italian Department of Civil Protection (DPC), and PON-AIM Ricerca e Innovazione 2014-2020 - Fondo Sociale Europeo, Azione I.2, "Smart, Secure and Inclusive Communities". These supports are gratefully acknowledged.

7. References

[1] Mehrabi AB, Shing PB, Schuller MP, Noland JL (1996): Experimental evaluation of masonry-infilled RC frames. *Journal of Structural Engineering*, **122** (3), 228-237

[2] Al-Chaar, G., Issa, M., Sweeney, S., 2002. Behavior of masonry-infilled non-ductile reinforced concrete frames. *Journal of Structural Engineering*, **128** (8), 1055-1063.

[3] Verderame GM, Ricci P, De Risi MT, Del Gaudio C (2019): Experimental Assessment and Numerical Modelling of Conforming and Non-Conforming RC Frames with and without Infills. *Journal of Earthquake Engineering*, doi: 10.1080/13632469.2019.1692098 (in press)

[4] Chrysostomou CZ, Asteris PG (2012): On the in-plane properties and capacities of infilled frames. *Engineering Structures*, **41**, 385-402.

[5] Ricci P, De Risi MT, Verderame GM, Manfredi G (2016): Procedures for calibration of linear models for damage limitation in design of masonry-infilled RC frames. *Earthquake Engineering and Structural Dynamics*, **45** (8), 1315-1335.

[6] De Risi MT, Del Gaudio C, Ricci P, Verderame GM (2018): In-plane behaviour and damage assessment of masonry in-fills with hollow clay bricks in RC frames. *Engineering Structures* **168** : 257–275.

[7] ASCE/SEI 41-06: Seismic rehabilitation of existing buildings. *American Society of Civil Engineers*, Reston, VA, USA, 2007.

[8] D.M. 2008, D.M. 14/01/2008. Approvazione delle nuove norme tecniche per le costruzioni. G.U. n. 29 del 4/2/2008. (in Italian)

[9] D.M. 2018, D.M. 17/01/2018. Aggiornamento delle nuove norme tecniche per le costruzioni. G.U. n. 42 del 20/2/2018. (in Italian)

[10] Crisafulli FJ (1997): Seismic behaviour of reinforced concrete structures with masonry infills, *PhD Thesis*, University of Canterbury, Canterbury, New Zealand.

[11] Burton H, Deierlein G (2014): Simulation of seismic collapse in non-ductile reinforced concrete frame buildings with masonry infills. *Journal of Structural Engineering*, 140 (SI: Computational simulation in structural engineering). **140**(8), A4014016.

[12] Sattar S, Liel AB (2015): Seismic performance of nonductile reinforced concrete frames with masonry infill walls: I. Development of a strut model enhanced by finite element models. *Earthquake Spectra*, **32**(2), 795-818.

[13] Jeon JS, Park JH, DesRoches R (2015): Seismic fragility of lightly reinforced concrete frames with masonry infills. *Earthquake Engineering & Structural Dynamics*, **44** (11), 1783-1803.

[14] Sezen H, Moehle JP (2004): Shear Strength Model for Lightly Reinforced Concrete Columns. *Journal of Structural Engineering*, Vol. **130**, No. 11.

[15] ASCE/SEI 41, Seismic evaluation and retrofit of existing buildings. American Society of Civil Engineers, Reston, VA, USA, 2017.

[16] Regio Decreto Legge n. 2229 del 16/11/1939. Norme per la esecuzione delle opere in conglomerate cementizio semplice od armato. G.U. n. 92 del 18/04/1940 (in Italian)

[17] ASTM C109/C109M-16a, Standard Test Method for Compressive Strength of Hydraulic Cement Mortars, ASTM International, West Conshohocken, PA, 2016, www.astm.org.

